IV Journeys in Multiphase Flows (JEM2017)
March 27-31, 2017 - São Paulo, Brazil

PaperID: JEM-2017-0054

A HEAT AND MASS TRANSFER MAPPING FOR THE $\mathrm{NH_3 - H_2O}$ AND $\mathrm{LiBr - H_2O}$ ABSORPTION REFRIGERATION SYSTEMS BASED ON THE FALLING FILM TECHNOLOGY

Beethoven Narváez-Romo
betonarmo@usp.br
SISEA, University of São Paulo, Brazil

José R. Simões-Moreira
jrsimoes@usp.br
SISEA, University of São Paulo, Brazil

Marx Chhay
marx.chhay@univ-savoie.fr
Université Savoie Mont Blanc

Eli W. Zavaleta-Aguilar
eli.zavaleta@itapeva.unesp.br
São Paulo State University (Unesp)

Abstract. *This paper presents a study of the heat and mass transfer behavior in falling liquid films technology for refrigeration ($T = 253[K]$) / air-conditioning ($T = 280[K]$) applications. Ammonia-water ($NH_3 - H_2O$) and Lithium bromide-water ($LiBr - H_2O$) absorption refrigeration cycles (ARC) have been simulated to find the typical operation condition, in which the mass and energy equations were implemented through the Engineering Equations Solver (EES). Heat and mass transfer correlations used in the absorption processes have been evaluated for both working fluid pairs, in which a mapping of the possible heat and mass transfer values is presented. The study allowed comparing the two technologies using the same operational conditions. The ascertainment that the transfer correlations may behave differently has been showed. Finally, the study suggests that future researches about heat and mass transfer behavior should be to carry out for realistic operational condition of the absorption refrigeration cycles.*

Keywords: *Heat and mass transfer, Absorption refrigeration, Ammonia-water, Lithium bromide-Water, Correlations*

1. INTRODUCTION

Edmond Carré developed the first absorption refrigeration machine in 1850 using a water and sulphuric acid (H_2SO_4) mixture as the working fluid pairs, requiring a large quantity of this salt to absorb a small quantity of water vapor in order to achieve the refrigeration process. However, in 1859, Ferdinand Carré used the ammonia-water pair as working fluid pairs, because of their properties: stability, low normal boiling point ($44°C$), and good ammonia affinity to water (Carmo Elvas *et al.*, 2010). Currently, lithium bromide-water and ammonia-water pair have been the most common working fluid pairs used in commercial absorption refrigeration cycles (ARC). The former operates in vacuum such as in Edmond Carré's machine, and the second one in a positive pressure such as in Ferdinand Carré 's machine.

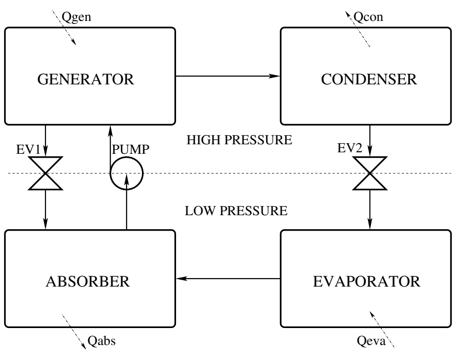

Figure 1. Absorption Refrigeration Cycle Diagram

An ARC is constituted by two pressure levels as depicted in Fig. (1); the low pressure level (evaporator and absorber) and the high pressure level (generator and condenser). These two levels are connected by two expansion valves (EV1 and EV2) and one solution pump, in its simplest configuration. The solution pump drives the strong liquid solution from the absorber to the generator in ammonia-water technology (or the weak liquid solution for the lithium bromide-water solution). At the generator, the solution flows over heated surface tubes in the falling film generator, whose function is to separate the refrigerant (ammonia or water vapor) from the liquid solution. Next, the vapor refrigerant is driven to the condenser, rejecting the heat to the environment, $\dot{Q}_{con}$. The condensed refrigerant reaches the evaporator, going through an expansion valve (EV2) reducing the pressure and the temperature by the Joule-Thomson effect to receive the heat load ($\dot{Q}_{eva}$) by evaporation. Next, the vapor refrigerant enters the absorber at the vapor state, in which it is absorbed by the weak solution (or strong for lithium bromide-water solution). Heat ($\dot{Q}_{abs}$) is rejected to an external coolant as the absorption process takes place, and then the solution is pumped to the generator closing the cycle.

It is worth mentioning that both the absorber and the generator are the main components of the absorption system because that there is a simultaneous heat and mass transfer process Yüksel and Schlünder (1987), in which the refrigerant changes phase Fujita (1993). In addition, the heat and mass transfer coefficients in those components are characterized by low values Castro *et al.* (2009). On the other hand, when ARC is compared with a vapor compression cycle (VCC), the former has lower coefficient of performance (COP), particularly if the absorption machine works beyond its design specifications. Therefore, enhancing the heat and mass transfer process leads to a reduction in costs and in the sorption machine size.

The current work aims the heat and mass transfer mapping in the falling liquid films technology for the absorption refrigeration systems in the refrigeration/air conditioning applications. Ammonia-water ($NH_3 - H_2O$) and Lithium bromide-water ($LiBr - H_2O$) absorption refrigeration cycles (ARC) have been simulated to find the typical operational condition, in which the mass and energy equations, thermophysical properties of mixtures and mean operational parameters were implemented through the *Engineering Equations Solver* - EES). Therefore, for these conditions, the heat and mass transfer correlations were evaluated as is represented in Fig. (2).

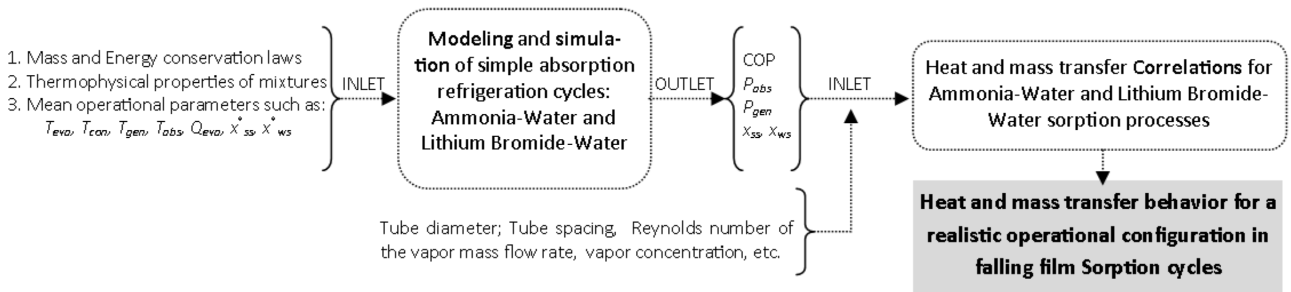

Figure 2. Method to evaluate the heat and mass transfer coefficient in a realistic sorption refrigeration cycles

2. Modeling and simulation of absorption refrigeration cycles

In this section, the absorption refrigeration modelization is presented, taking into account all components of the cycle such as generator, rectifier (for ($NH_3 - H_2O$) only), condenser, expansion valves, evaporator, absorber, and pump. Each one was analyzed as an independent control volume, in which the mass, component mass and energy equations were developed in a steady-stage regime. Next, the ammonia-water absorption refrigeration cycle will be analyzed.

2.1 Ammonia-water absorption refrigeration cycle

ARC modelization requires deep attention at the most critical processes such as generation and absorption processes due to simultaneous heat and mass transfer. Therefore, these components are analyzed as is shown in Fig. (3).

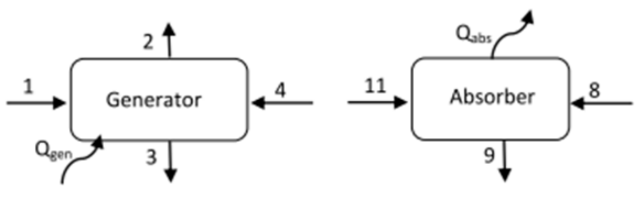

Figure 3. Control volume for the generation and the absorption process

The falling film generator is employed to separate the ammonia (2-label) from the ammonia-water strong solution (1-label) when a heat source is applied (Q_{gen}), in which the weak solution is the remaining solution after the separation process (3-label). The rectifier is used to purify the ammonia vapor and hence that condensed goes back to the generator (4-label). On the other hand, the falling film absorber is used to absorb the ammonia vapor coming of the evaporator (8-label) into the weak ammonia-water solution (11-label) that comes of the generator, and then the strong ammonia-water solution (9-label) is obtained, as shown in Fig. (3). The mass, ammonia mass, and energy equations are given by Eqs. (1-3) and by Eqs. (4-6) for the generation and absorption processes, respectively; while $\dot{m}$, i and x are the mass flow rate, specific enthalpy and the ammonia mass fraction, respectively.

$$\dot{m}_3 + \dot{m}_2 = \dot{m}_1 + \dot{m}_4 \tag{1}$$

$$\dot{Q}_{gen} = \dot{m}_2 i_2 + \dot{m}_3 i_3 - \dot{m}_1 i_1 - \dot{m}_4 i_4 \tag{2}$$

$$\dot{m}_3 x_3 + \dot{m}_2 x_2 = \dot{m}_1 x_1 + \dot{m}_4 x_4 \tag{3}$$

$$\dot{m}_{11} + \dot{m}_8 = \dot{m}_9 \tag{4}$$

$$\dot{Q}_{abs} = \dot{m}_8 i_8 + \dot{m}_{11} i_{11} - \dot{m}_9 i_9 \tag{5}$$

$$\dot{m}_{11} x_{11} + \dot{m}_8 x_8 = \dot{m}_9 x_9 \tag{6}$$

Several simplified hypothesis were carried out to solve the whole equation system such as; (1) condensation temperature, $T_6 = 313.15K$, (2) evaporation temperature, $T_8 = 280.15K$, (c) thermal load, $\dot{Q}_{eva} = 3.517[kW]$[1], (d) generation temperature, $T_3 = 373.15K$, and (e) absorption temperature, $T_9 = 298.15K$. In addition, other assumptions were carried out to simplify the system, (a) quality equal to $q_u = 0$ - saturated liquid- in the 3, 4, 6 and 9 points; (b) quality equal to $q_u = 1$ saturated vapor- in the 2, 5 and 8 points; (b) two pressure levels only: high pressure level in the 1, 2, 3, 4, 5, 6, 11 and 12, low pressure level in the 7, 8, 9 and 10 points; (c) generation process occurs in thermodynamic equilibrium, $T_3 = T_2$; (d) the temperature in the point 4 is computed by the arithmetic mean, $T_4 = 0.5 * (T_2 + T_5)$ Herold *et al.* (2016), (e) heat exchanger with infinity area, $Q_{subcool} = Q_{pre-heat}$, $T_{11} = T_{12}$, and (f) isentropic pumping. Fig. (4) shows the numerical results of the whole operational parameters such as ammonia-mass fraction (x), absorption pressure (P_{abs}) and generation pressure (P_{gen}), mass flow rate ($\dot{m}$), just to mention a few.

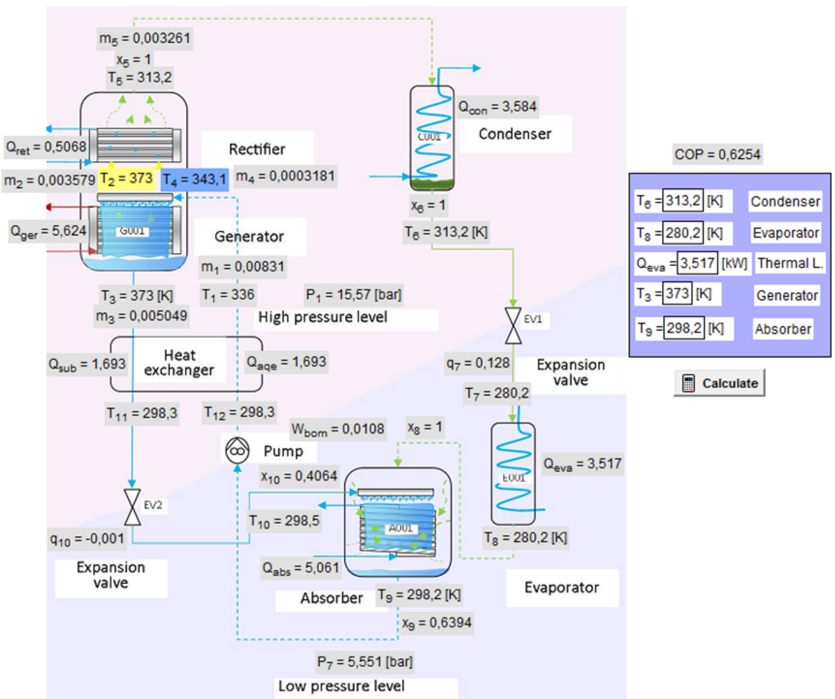

Figure 4. Results of the simulation of the ammonia-water absorption refrigeration cycle

However, some parameters have been adjusted to cover the operation ranges applied in refrigeration/air conditioning systems. The simulation was carried out for two evaporation temperatures; $T_{eva} = 253[K]$ for refrigeration applications and $T_{eva} = 280[K]$ for air condition systems, two condensation temperatures ($T_{con} = 303$ and $T_{con} = 313[K]$), and two generation temperatures ($T_{gen} = 373$ and $T_{gen} = 393[K]$), aiming to achieve typical operation conditions. All the simulation results are showed in Table (1) such as the coefficient of performance (COP), absorption pressure (P_{abs}), generation pressure (P_{gen}), strong solution concentration (x_{ss}), weak solution concentration (x_{ws}). In addition, the Prandtl number (Pr) and Schmidt number were computed (Sc).

[1]Thermal load was necessary to run the model, however, the thermal load affect directly the equipment size

Table 1. Operational conditions of the ammonia-water absorption refrigation cycle

Cond.	$T_{con}, [K]$	$T_{eva}, [K]$	$T_{gen}, [K]$	COP	$P_{abs}, [bar]$	$P_{gen}, [bar]$	$x_{ss}, [-]$	$x_{ws}, [-]$	Pr	Sc
1	313	280	373	0.6245	5.51	15.49	63.72	40.52	1.64	14.4
2	313	280	393	0.5157	5.51	15.49	63.72	31.41	1.91	21.5
3	313	253	373	0.5547	1.88	15.49	41.51	40.52	2.29	37.3
4	313	253	393	0.4606	1.88	15.49	41.51	31.41	2.63	52.4
5	303	280	373	0.6083	5.51	11.62	63.72	34.54	1.82	18.9
6	303	280	393	0.4779	5.51	11.62	63.72	25.78	2.1	27.4
7	303	253	373	0.5407	1.88	11.62	41.51	34.54	2.52	46.9
8	303	253	393	0.4298	1.88	11.62	41.51	25.78	2.87	64.2

2.2 Lithium bromide-water absorption refrigeration cycle

For lithium bromide-water working fluid, the operation conditions were also defined by the same previous analysis. The results are showed in Fig. (5), in which the lithium bromide concentrations were defined at the design specifications using the crystallization limit to define the weak solution concentration. The generator temperature was declared as a function of the weak and strong liquid concentration, turning out as a dependent variable. Evaporation temperature was only evaluated at $7°C$ due to refrigerant properties (water). Therefore, this technology is widely used in air conditioning applications. All the results are showed in Tab. (2), in which the first and second column represent the condensation temperature (T_{con}) and evaporation temperature (T_{eva}), respectively; while x_{ss}, x_{ws} are the strong and weak solution, respectively. Next, the coefficient of performance (COP), absorption pressure (P_{abs}), generation pressure (P_{gen}), generation temperature (T_{gen}). Finally, the Prandtl number (Pr) and Schmidt number (Sc) are computed.

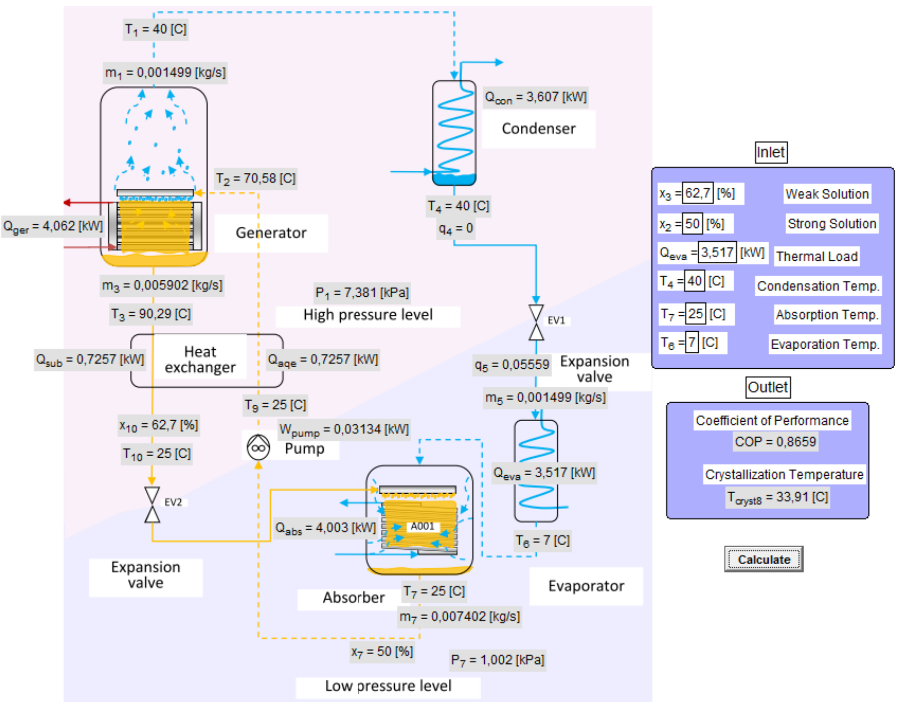

Figure 5. Results of the simulation of the lithium bromide-water absorption refrigeration cycle

Table 2. Operational conditions of the lithium bromide-water absorption refrigeration cycle

Cond.	$T_{con}, [K]$	$T_{eva}, [K]$	$x_{ss}, [-]$	$x_{ws}, [-]$	COP	$P_{abs}, [kPa]$	$P_{gen}, [bar]$	$T_{gen}, [-]$	Pr	Sc
1	313	280	50	62.7	0.8659	1	7.38	90.29	24.17	2101
2	303	280	50	62.7	0.883	1	4.25	78.43	24.17	2101

3. Heat and mass transfer correlations in falling film technology

Nusselt (1916) analyzed the isothermal condensation phenomenon on a flat plate for a pure substance, assuming: laminar regime, Newtonian fluid, constant properties, and without inertial forces from the vapor acting at the interface, obtaining an expression of the average heat transfer coefficient, h_l, as a function of the acceleration of gravity, g, the Reynolds number, Re, and the fluid properties; dynamic viscosity, μ, density, ρ, and the liquid thermal conductivity k. Hence, the Nusselt number for this case is defined by Eq. (7). In addition, the dimensionless Sherwood number is expressed by Eq. (8)

$$Nu = \frac{h_l}{k}\left(\frac{\nu^2}{g}\right)^{1/3} = 1.467Re^{-1/3} \tag{7}$$

$$Sh = \frac{k_m}{D_m}\left(\frac{\nu^2}{g}\right)^{1/3} \tag{8}$$

Table 3. Application range of the ammonia-water correlations

Author	Correlation	*Pr*	*Re*	*Sc*	*T*,°C	*P*,*kPa*	*x*, % *y*, %	Remarks
Bohra (2007)	9, 10	2.2-10.4 $0.5-0.93$	$26-157$ -	$45.4-588.1$ $0.5-0.53$	$14.8-105.4$ $(-10.5)-28.2$	$169-520$	$5;15;25;40$ -	
Jeong *et al.* (1998)	17	$2.4-3.9$ -	$20-300$ -	-	$45-54$ $66-69$	$67-117$	$1.2;3.7$ $63;77$	
T. Kang *et al.* (1999)	13, 14	$3.8-5.8$ -	$17-24$ -	$33.8-39.2$ -	$17.0-37.2$ $54.5-66.5$	101.3	$5;10;15$ $64.7-79.7$	
Kwon and Jeong (2004)	18	$2.1-3.8$ -	$10-250$ -	-	$45-60$ -	$17-193$	$3;14;30$ $45.6;84.4;96.5$	
Lee (2007)	11, 12	$2.2-8.2$ $0.5-0.93$	$29.7-169.2$ -	$43.6-362.7$ $0.5-0.53$	$14.8-105.4$ $(-10.5)-28.2$	$169-520$	$5;15;25;40$ -	$Gr_v = 4223-59893$ $Ja_v = 0.0098-0.0387$
Lee *et al.* (2002a)	15, 16	$3.8-5.8$ $-$	$50-700$ $25-200$		$15.5-20$ $-$	101.3	$0.1-0.3$ $-$	

3.1 Correlations involving ammonia-water solution for the absorption processes

Correlations involving ammonia-water solutions are presented, i.e, Bohra (2007) Eqs. (9, 10), Lee (2007) Eqs. (11, 12), T. Kang *et al.* (1999) Eqs. (13, 14), Lee *et al.* (2002a) Eqs.(15, 16), Jeong *et al.* (1998) Eqs.(17), Kwon and Jeong (2004) Eq. (18). All the correlations were obtained in falling film technology for the absorption refrigeration cycle in the ammonia-water solution. Fig. (6) shows the Sherwood number as a function of the Reynolds number, whose mass transfer is enhanced as the Reynolds number is increased. However, the mass transfer coefficient will strongly enhance as the absorption refrigeration cycle achieves evaporation temperatures below $0°C$. Moreover, Fig. (6) displays the possible mass transfer mapping for the absorption refrigeration cycle for the whole operational conditions given in Tab. (1). The mass transfer mapping of Bohra (2007) agree with Lee (2007). However, T. Kang *et al.* (1999) underestimates these values, in which it may be explained by the conditions that the experiments were carried out at the test rig (low purity of ammonia vapor). Therefore, the Sherwood number in refrigeration/air conditioning applications may vary from 0.015 to 0.08. The operational conditions 2 to 7 were not shown in Fig. (6), but these values are found in Tab. (1), and in Tab. (3) the application range of these correlations are displayed.

$$Nu_{seg,\delta} = 7.589 \cdot 10^{-3} Re^{1.04} Pr^{0.45} \left(\frac{P_{abs}}{345kPa}\right)^{-0.145} \tag{9}$$

$$Sh_{seg,\delta} = 1.298 \cdot 10^{-4} Re^{0.57} Sc^{1.32} \left(\frac{P_{abs}}{345kPa}\right)^{0.644} \tag{10}$$

$$Nu_{\delta} = 3.22 \cdot 10^{-3} Re^{0.945} Pr^{0.743} \left(\frac{P_{abs}}{345kPa}\right)^{-0.269} \tag{11}$$

$$Sh_{\delta} = 7.437 \cdot 10^{-4} Re^{0.397} Sc^{1.04} \left(\frac{P_{abs}}{345kPa}\right)^{0.8841} \tag{12}$$

$$Nu = 0.8530 \cdot 10^{-3} Re_l^{1.518} Re_v^{0.1759} \left(\frac{T_v - T_l}{T_l}\right)_i^{1.8790} \left(\frac{x_v - x_l}{x_l}\right)_i^{-0.5756} \tag{13}$$

$$Sh = 0.6996 \cdot 10^{-7} Re_l^{0.8874} Re_v^{1.265} \left(\frac{T_v - T_l}{T_l}\right)_i^{0.8844} \left(\frac{x_v - x_l}{x_l}\right)_i^{0.5304} \tag{14}$$

$$Nu = 0.01369 Re_l^{0.5103} Re_v^{0.02461} \left(\frac{T_v - T_l}{T_l}\right)_i^{0.2977} \left(\frac{x_v - x_l}{x_l}\right)_i^{0.1438} \tag{15}$$

$$Sh = 658.46 Re_l^{0.0195} Re_v^{0.9571} \left(\frac{x_v - x_l}{x_l}\right)_i^{-0.0639} \tag{16}$$

$$Nu = 0.00022 Re \quad 50 \leq Re \leq 300 \tag{17}$$

$$Nu = 1.683 \cdot 10^{-4} Re_l^{0.8672} \tau_v^{*-0.3018} \tag{18}$$

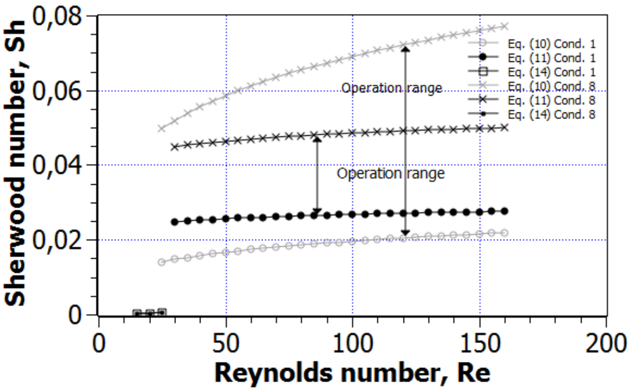

Figure 6. Sherwood number as a function of the Reynolds number for the ammonia-water solution

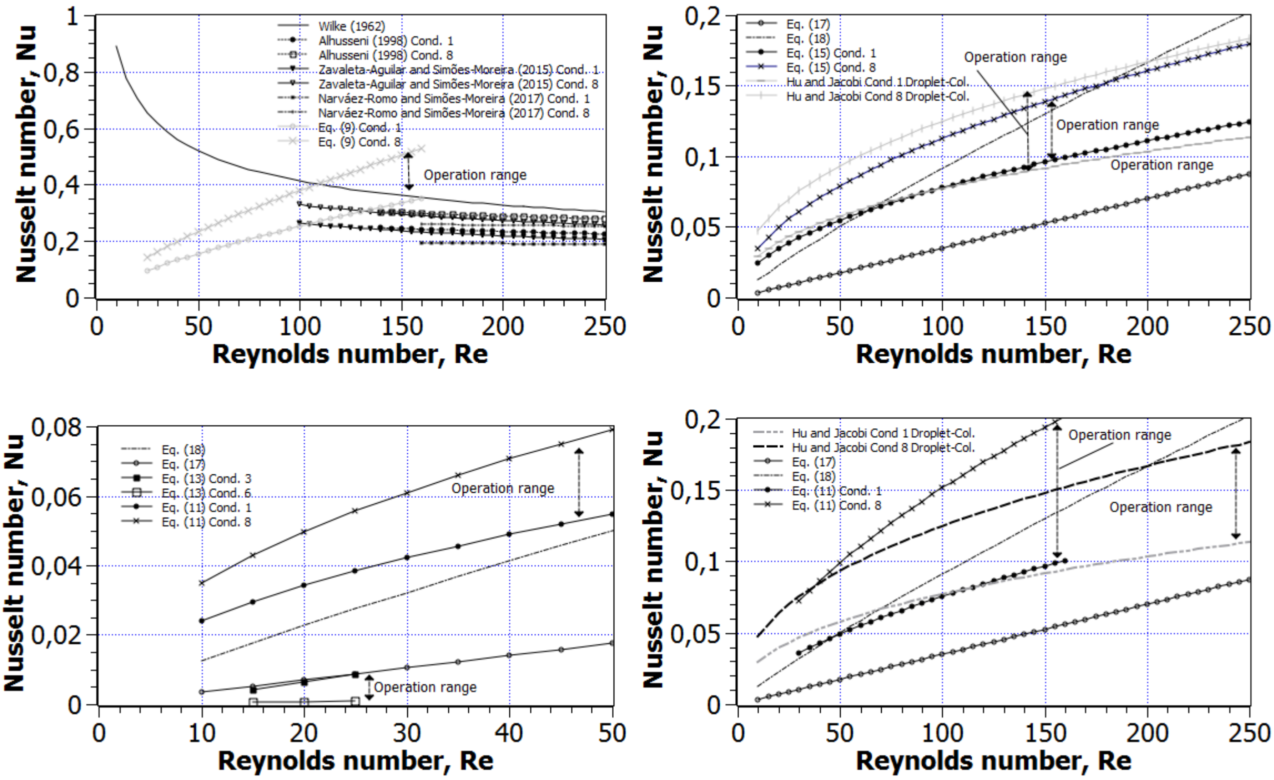

Figure 7. Nusselt as a function of the Reynolds number for the ammonia-water solution

Fig. (7) shows the Nusselt number as a function of the Reynolds number. The first Fig. (upper-left side) displays the correlations used in the falling film technology using other working fluids for an evaporation process, in which these correlations such as Narváez-Romo and Simões-Moreira (2017), Zavaleta-Aguilar and Simões-Moreira (2015), Wilke (1962) and Alhusseini *et al.* (1998) show similar heat transfer values from Bohra (2007) for the Reynolds numbers between 100 and 150. However, the fashion curves of these processes are opposite. The second Fig. (upper-right side) displays a comparison between Jeong *et al.* (1998), Kwon and Jeong (2004), Lee *et al.* (2002b) and Hu and Jacobi (1996), showing that these expressions present similar results each other, i.e., Kwon and Jeong (2004) expression found inside the operating range of Lee *et al.* (2002b) and Hu and Jacobi (1996). Therefore, the Hu and Jacobi (1996) expression may be used to design the absorption process (droplet-column pattern flow). However, Jeong *et al.* (1998) underestimates the heat transfer due to this expression neglects the effects taken into account by the Prandtl number. The third Fig. (bottom-left side) compares the expressions of Kwon and Jeong (2004), Lee (2007), Jeong *et al.* (1998), and T. Kang *et al.* (1999), showing the behavior of the Nusselt number for low Reynolds numbers (10 to 50). T. Kang *et al.* (1999) underestimates the Nusselt number as the Reynolds number increases. Finally, the last Fig. (bottom-right side) correlate the expressions of Jeong *et al.* (1998), Kwon and Jeong (2004), Lee (2007) and Hu and Jacobi (1996), in which all the correlations have a good agreement. Therefore, Fig. (7) shows that the Nusselt number may be vary between 0.001 and $0,2$ for the Reynolds number ranged from 10 to 250 (with an exception of Bohra (2007)). It is worthwhile to mention that the best performance of the heat transfer is achieved at the lowest evaporation temperature ($T_{eva} = 253[K]$) for all the correlations.

3.2 Correlations involving lithium bromide-water solution for absorption processes

For lithium bromide-water there are several expressions; Kim and Infante Ferreira (2008) studied the heat and mass transfer with four different liquid films in which pure water and a 50% LiBr solution, with or without 100 ppm of 2-ethyl-1-hexanol (2-EH) as additive were used, being Eqs. (19, 20) with solution and bare; Eqs. (21, 22) with solution and screen; Eqs. (23, 24) with solution, 2-ethyl glycol and bare; Eqs. (25, 26) with solution, 2-ethyl glycol and screen; Karami and Farhanieh (2009) and Karami and Farhanieh (2011) obtained the follow expressions; Eqs. (27-30); Finally, Babadi and Farhanieh (2005) found the Eqs. (31-32). Fig. (8) shows the Sherwood number as a function of the Reynolds number, in which the expressions display different behavior for the same operational conditions, i.e., Karami and Farhanieh (2009) and Karami and Farhanieh (2011) show a strong dependence of the Sherwood number as the Reynolds number changes, enhancing the mass transfer as the Reynolds number increases. In contrast, Kim and Infante Ferreira (2008) show that the increase of the Reynolds number diminishes the Sherwood number. It is worthwhile to mention that the Kim and Infante Ferreira (2008) expressions were experimentally obtained. On the other hand, Babadi and Farhanieh (2005) underestimates the Sherwood number as compared with Kim and Infante Ferreira (2008), Karami and Farhanieh (2009) and Karami and Farhanieh (2011). Fig. (9) shows the behavior of the Nusselt number as a function of the Reynolds number, in which the heat transfer improves as the Reynolds number increases. Nevertheless, the expressions of Babadi and Farhanieh (2005) and Karami and Farhanieh (2009) shows an opposite behavior.

Table 4. Application range of the lithium bromide-water correlations

Author	**Correlation**	***Pr***	***Re***	***T*,°C**	***P,kPa***	***x***	**Remarks**
Babadi and Farhanieh (2005)	31 - 32	28.5	$5-100$	40	1	62	
Karami and Farhanieh (2009)	27, 28	17.7	$5-150$	45	1	60	
Karami and Farhanieh (2011)	29, 30	17.7	$5-150$	45	1	60	Inclined plate
Kim and Infante Ferreira (2008)	19 - 26	$\cong 11-15$	$40-110$	$18-42$	$0.7-2.9$	50	

$$Nu = 0.0249 Re_l^{0.069} Pr_l^{0.5} \tag{19}$$

$$Sh = 0.896 Re_l^{-0.3} Sc_l^{0.5} \tag{20}$$

$$Nu = 0.00493 Re_l^{0.469} Pr_l^{0.5} \tag{21}$$

$$Sh = 0.965 Re_l^{-0.343} Sc_l^{0.5} \tag{22}$$

$$Nu = 0.0259 Re_l^{0.247} Pr_l^{0.5} \tag{23}$$

$$Sh = 2.623 Re_l^{-0.265} Sc_l^{0.5} \tag{24}$$

$$Nu = 0.0166 Re_l^{0.279} Pr_l^{0.5} \tag{25}$$

$$Sh = 0.886 Re_l^{-0.24} Sc_l^{0.5} \tag{26}$$

$$Nu_\delta = 0.4767 Re_l^{0.0477} Pr_l^{0.334} \tag{27}$$

$$Sh_\delta = 0.1329 Re_l^{1.0571} Sc_l^{0.334} \tag{28}$$

$$Nu_\delta = 0.024 Re_l^{0.464} Pr_l^{0.334} \tag{29}$$

$$Sh_\delta = 0.1329 Re_l^{1.13} Sc_l^{0.334} \tag{30}$$

$$Nu = 0.45 Re_l^{-0,23} Pr_l^{0.33} \quad \text{for} \quad Re < 60 \tag{31}$$

$$Sh = 1.03 Re_l^{-0.146} \left(\frac{Sc_l}{1000}\right)^{1.42} \quad \text{for} \quad Re < \left(\frac{Sc_l}{5367}\right)^{-3.61} \tag{32}$$

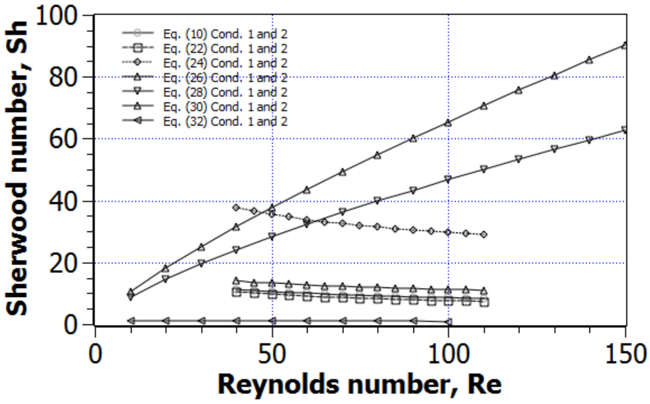

Figure 8. Sherwood number as a function of the Reynolds number for the Lithium bromide-water solution

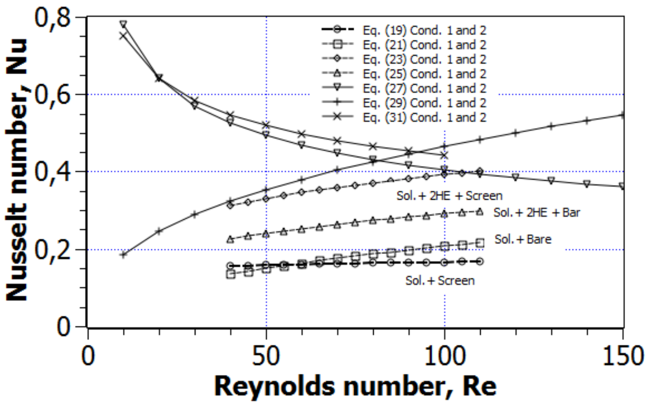

Figure 9. Nusselt number as a function of the Reynolds number for the Lithium bromide-water solution

4. CONCLUSIONS

In this communication, a review study on heat and mass transfer correlations was presented. The transfer correlations deal with sorption machine using falling film technology with an ammonia-water solution or lithium bromide-water solution. The heat and mass transfer of the Ammonia-water and Lithium bromide-Water absorption refrigeration cycles were compared, showing a mapping of the possible heat and mass transfer values focused in refrigeration/air conditioning applications. In addition, the study defined the limitations of the conventional expressions at the design of the absorption processes. The review summarizes the operating range of each correlation within tables. A graphical comparison of the transfer correlations is performed for a given operation condition. The ascertainment that the transfer correlations may behave differently demonstrate that further studies have to be performed, specifically to implement the correlations into a more realistic operational configurations related to sorption machine.

5. ACKNOWLEDGEMENTS

The first author thanks to Fundación CEIBA and CNPq for the financial support.

6. REFERENCES

Alhusseini, A.A., Tuzla, K. and Chen, J.C., 1998. "Falling film evaporation of single component liquids". *Int. J. Heat Mass Transfer*, Vol. 41, No. 12, pp. 1623–1632.

Babadi, F. and Farhanieh, B., 2005. "Characteristics of heat and mass transfer in vapor absorption of falling film flow on a horizontal tube". *Int. Commun. Heat Mass*, Vol. 32, No. 9, pp. 1253–1265. ISSN 07351933. doi: 10.1016/j.icheatmasstransfer.2005.05.011.

Bohra, L.K., 2007. *Analysis of binary fluid heat and mass transfer in ammonia-water absorption*. Ph.D. thesis, Georgia Institute of Tecnhology.

Carmo Elvas, M., Perez, M.I. and Carvalho, S., 2010. "Making science cooler: Carré's apparatus". In *International Conference of ESHS*. pp. 441–449.

Castro, J., Oliet, C., Rodríguez, I. and Oliva, A., 2009. "Comparison of the performance of falling film and bubble absorbers for air-cooled absorption systems". *Int. J. Therm. Sci.*, Vol. 48, No. 7, pp. 1355–1366. ISSN 12900729.

Fujita, T., 1993. "Falling liquid films in absorption machines". *Int. J. Refrigeration*, Vol. 16, No. 4, pp. 282–294. ISSN 01407007.

Herold, K.E., Radermacher, R. and Klein, S.A., 2016. *Absorption chillers and heat pumps*. CRC press.

Hu, X. and Jacobi, A., 1996. "The intertube falling film: Part 1âĂŤflow characteristics, mode transitions, and hysteresis". *J. Heat Transfer*, Vol. 118, No. 3, pp. 616–625.

Jeong, S., Lee, S.K., Koo, K.K., Ziegler, F. *et al.*, 1998. "Heat transfer performance of a coiled tube absorber with working fluid of ammonia/water/discussion". *ASHRAE Transactions*, Vol. 104, p. 1577.

Karami, S. and Farhanieh, B., 2009. "A numerical study on the absorption of water vapor into a film of aqueous LiBr falling along a vertical plate". *Heat and Mass Transfer/Waerme- und Stoffuebertragung*, Vol. 46, No. 2, pp. 197–207. ISSN 09477411.

Karami, S. and Farhanieh, B., 2011. "Numerical modeling of incline plate LiBr absorber". *Heat and Mass Transfer/Waerme- und Stoffuebertragung*, Vol. 47, No. 3, pp. 259–267. ISSN 09477411.

Kim, D.S. and Infante Ferreira, C.a., 2008. "Flow patterns and heat and mass transfer coefficients of low Reynolds number falling film flows on vertical plates: Effects of a wire screen and an additive". *Int. J. Refrigeration*, Vol. 32, No. 1, pp. 138–149. ISSN 01407007.

Kwon, K. and Jeong, S., 2004. "Effect of vapor flow on the falling-film heat and mass transfer of the ammonia/water absorber". *Int. J. Refrigeration*, Vol. 27, No. 8, pp. 955–964. ISSN 01407007.

Lee, K.B., Chun, B.H., Lee, J.C., Hyun, J.C. and Kim, S.H., 2002a. "Comparison of heat and mass transfer in falling film and bubble absorbers of ammonia water". , No. September 2001, pp. 191–205.

Lee, K.B., Chun, B.H., Lee, J.C., Lee, C.H. and Kim, S.H., 2002b. "Experimental analysis of bubble mode in a plate-type absorber". *Chem. Eng. Sci.*, Vol. 57, No. 11, pp. 1923–1929. ISSN 00092509. doi:10.1016/S0009-2509(02)00089-1.

Lee, S., 2007. *Development of techniques for in-situ measurement of heat and mass transfer in ammonia-water absorption systems*. Ph.D. thesis, Georgia Institute of Tecnhology.

Narváez-Romo, B. and Simões-Moreira, J.R., 2017. "Falling liquid film evaporation in subcooled and saturated water over horizontal heated tubes". *Heat Transfer Engineering*, Vol. 38, No. 3, pp. 361–376.

Nusselt, W., 1916. "Die oberflachenkondesation des wasserdamffes the surface condensation of water". *Zetrschr. Ver. Deutch. Ing.*, Vol. 60, pp. 541–546.

T. Kang, Y., Akisawa, A. and Kashiwagi, T., 1999. "Experimental correlation of combined heat and mass transfer for NH3-H2O falling film absorption.pdf". *Int. J. Refrigeration*, Vol. 22, pp. 250–262.

Wilke, W., 1962. "Warmeubertragung an rieselfilme (heat transfer to falling liquid films)". *VDI-Forschungsheft*, Vol. 490, p. B28.

Yüksel, M. and Schlünder, E., 1987. "Heat and mass transfer in non-isothermal absorption of gases in falling liquid films". *Chem. Eng. Process. Process Intensification*, Vol. 22, No. 4, pp. 193–202. ISSN 02552701.

Zavaleta-Aguilar, E. and Simões-Moreira, J., 2015. "Horizontal tube bundle falling film distiller for ammonia–water mixtures". *Int. J. Refrigeration*, Vol. 59, pp. 304–316.

7. RESPONSIBILITY NOTICE

The authors are the only responsible for the printed material included in this paper.